

Glass transition and random close packing in 3+ dimensions

Patrick Charbonneau,¹ Atsushi Ikeda,² Giorgio Parisi,³ and Francesco Zamponi⁴

¹*Departments of Chemistry and Physics, Duke University, Durham, North Carolina 27708, USA**

²*Laboratoire Charles Coulomb, UMR 5221 CNRS and Université Montpellier 2, Montpellier, France*

³*Dipartimento di Fisica, Sapienza Università di Roma, INFN,*

Sezione di Roma I, IPFC – CNR, P.le A. Moro 2, I-00185 Roma, Italy

⁴*LPT, École Normale Supérieure, UMR 8549 CNRS, 24 Rue Lhomond, 75005 France*

Motivated by a recently identified severe discrepancy between a static and a dynamic mean-field theory of glasses, we numerically investigate the behavior of dense hard spheres in spatial dimensions 3 to 12. Our results are consistent with the static replica theory, but disagree with the dynamic mode-coupling theory, indicating that some key ingredients are missing from the latter. We also obtain numerical estimates of the random close packing density, which provides new insights into the mathematical problem of packing spheres in large dimension.

Over the last century, the study of physical theories upon varying the dimensionality of space d has illuminated a variety of problems. Unifying fundamental forces through general relativity and string theories immediately come to mind, but so does the treatment of critical phenomena through the renormalization group approach. Similar contemplations may now benefit another grand challenge of condensed matter, that of describing glass formation [1]. Including d within the set of control parameters may indeed nicely complement two- and three-dimensional experiments and simulations by, on the one hand, surmounting some of the technical challenges encountered in low dimensions [2]; and, on the other hand, by bringing the problem in contact with rich mathematical fields, such as coding theory [3]. Obtaining a complete and consistent high-dimensional theory of amorphous states would also crucially pave the way for a more systematic understanding of finite dimensional effects, and ultimately provide a reliable theory of the glass transition, of jamming, and of related phenomena.

The Random First Order Transition (RFOT) theory has emerged as one of the main contenders in the quest for a complete description of the glass transition. Its foundation was posed in the late eighties, when it was realized that a class of mean-field spin models share the phenomenology of glass formers [4]. These models are very abstract and do not obviously present the microscopic features of particle-based systems, but they helped turn RFOT theory into a quantitative method for studying glasses, thanks to the development of the static replica theory (RT) [5] and the dynamic mode-coupling theory (MCT) [6]. The two quantitative theories of the glass transition are thus intimately related [7, 8]. However, MCT and RT make use of different approximations in order to obtain closed-form structures [8], which may lead to diverging physical descriptions. Indeed, the predictions of MCT [9, 10] and RT [11] strongly disagree in the limit of large d , and MCT predicts that the glass transition happens at a density that is much larger than the random close packing density predicted by RT. This is particularly worrying [12]. Because RFOT theory is

based on a mean-field description, it should be exact in large d , and MCT and RT should then lead to identical predictions, as already noted in [7]. In order to test the quality of the approximations and to clarify the connection with the original mean-field models, one ought to understand the source of the discrepancy, and to obtain a controlled limit of particle systems in which RFOT becomes exact. In other words, in order for further progress on the glass problem to be made, the dimensional question has to be resolved.

Independently from this issue, packing spheres in high dimension is intimately related to several important mathematical problems, notably in the context of signal digitalization and of error correcting codes [3]. It has been suggested that for large d , disordered packings may be more efficient than lattice-based versions [13]. Although lattice geometries are strongly d dependent, the fluid structure and properties have been suggested to be much less sensitive to d , once $d \gtrsim 3$ (see e.g. Ref. [14]). A general understanding of disordered packings in arbitrary d would thus also clarify the density scaling of amorphous packings and their potential mathematical role.

In this letter, we compare simulations of hard spheres up to $d = 12$ with the predictions of RT and MCT. The results suggest that while RT offers a satisfying description of dimensionality MCT fails at the task, which calls for a modified formulation of the dynamical theory of RFOT. The results also provide the “random close-packed” density in several d and give a hint of the scaling of this quantity for large d , which should allow comparisons with the results of other theoretical treatments [15].

Numerical simulations - For the simulation approach, we employ a modified Lubachevsky-Stillinger algorithm to densify a low-density gas of N identical hard spheres of diameter σ , enclosed in a periodic box of volume V , by growing the particles at a constant rate $\gamma = \dot{\sigma}$, reported here in standard reduced units [16, 17]. Time evolution stops when the system reaches a high reduced pressure $p \equiv \beta P / \rho = 10^3$ measured by rescaling the mechanical pressure P by the number density $\rho \equiv N/V$ and the inverse temperature β , which is thermostated

to unity. Our event-driven molecular dynamics scheme complements Ref. [16]’s earlier implementation of cubic blocking of space with spherical nearest-neighbor lists. Because the volume of a ball inscribed in a cube tends to zero with growing d , remarkable efficiency gains are obtained from considering collisions with fewer neighbors. Up to $d = 10$, particles are grown at rates as low as $\gamma = 3 \times 10^{-5}$, while rates of 3×10^{-4} and 10^{-2} are attained in $d = 11$ and 12, respectively. Systems containing $N = 8000$ particles are considered up to $d = 9$ and larger ones for $d = 10$ –12 [19]. These sizes ensure that even when the system is at its most dense the box edge remains larger than 2σ , which prevents a particle from ever having two direct contacts with another one. There are strong reasons to believe that although relatively small these N nonetheless provide a reliable approximation of bulk behavior. First, with increasing d the box side becomes less representative of the overall box dimension. The largest diagonals are \sqrt{d} larger and there are many more diagonals than box sides. Second, by analogy to spin systems, mean-field arguments indicate that for $d \rightarrow \infty$, a hypercube of side two is sufficient to capture the full thermodynamic behavior. Even at the critical point, finite-size corrections are proportional to $1/N^\delta$, where the exponent δ is model dependent (e.g. $1/2$ at the ferromagnetic transition), and not to the linear box length [20]. Similar results hold for dimensions greater than the upper critical dimension, where the exponents coincide with the mean field ones. Third, the fluid structure is expected to become uniform at ever smaller distances with increasing d [16, 18]. Nearest-neighbor ordering should thus mainly be influenced by particles in contact or nearly so, with the rest of the fluid acting as a continuum. Indeed, in the fluid phase, finite volume corrections are proportional to the pair correlation $h(L)$ for boxes of side L , and at fixed L , $h(L)$ goes to zero exponentially with d [18]. Finally, we satisfactorily test the validity of these rationalizations by a direct numerical investigation of finite size effects for $d = 8$ systems [19].

Numerical results - The compression results for $d = 9$ shown in Fig. 1 are representative of the behavior observed for all dimensions except $d = 3$, where crystallization is observed at small γ [16]. The system first follows the equilibrium fluid equation of state (EOS) at low density and falls out of equilibrium at high density. Beyond this point, the pressure increases faster than in the equilibrium fluid and ultimately diverges at packing fraction $\varphi_j(\gamma)$. A Carnahan-Starling form

$$p_{\text{fluid}}(\varphi) = 1 + 2^{d-1} \varphi \frac{1 - A_d \varphi}{(1 - \varphi)^d}, \quad (1)$$

captures well the pressure growth with φ in the fluid regime (Fig. 1), provided, for each dimension, that one fits A_d to the data from the slowest compression rate available [21]. Note that the coefficients A_d^{fit} are not identical to A_d^{CS} adjusted to recover the correct third virial

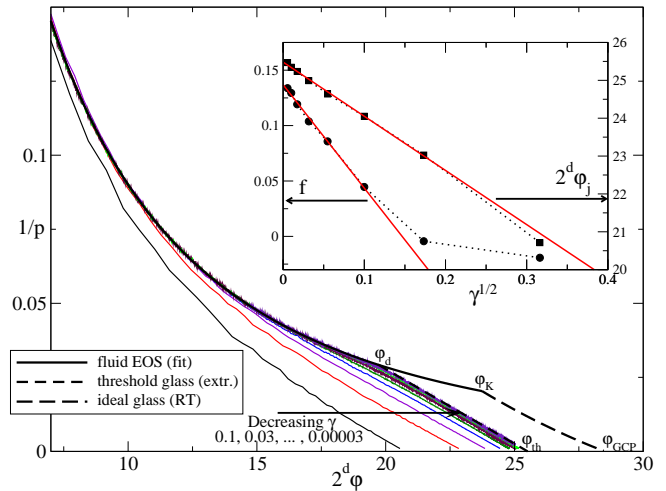


FIG. 1: Different compactions of $N = 8000$ particles in $d = 9$. With growing packing fraction $\varphi \equiv \rho V_d(\sigma/2)$, where $V_d(R)$ is the volume of a d -dimensional ball of radius R , the pressure first evolves like the fluid EOS then like a free volume EOS. Extrapolated threshold glass and theoretical ideal glass lines illustrate the subsequent analysis (see text for details).

coefficient [22] (Table II of [19]). The values, however, are quite close and this contribution in any case vanishes with increasing d .

In the high-density non-equilibrium regime, compaction runs with different γ follow separate branches along which the pressure evolution is dominated by the expulsion of free volume [23, 24]. Upon approaching jamming, the pressure is well approximated by

$$p_{\text{fv}}(\gamma, \varphi) = \frac{d \varphi_j(\gamma) [1 - f(\gamma)]}{\varphi_j(\gamma) - \varphi}, \quad (2)$$

where both $f(\gamma)$ and $\varphi_j(\gamma)$ are extracted from fitting the simulation data for $p \geq p_{\text{min}}$ (Table II of [19]). Very close to jamming ($p \gtrsim 10^5$), $f(\gamma)$ can be interpreted as the fraction of “rattlers” present, but in the regime where the fluid first becomes non-ergodic, caging heterogeneity results in a larger effective f [23]. We find that with decreasing γ , $f(\gamma)$ converges to values of order 10%, with only a weak d dependence (Fig. 1).

Data analysis - The numerical results qualitatively agree with the RFOT scenario (see Ref. [11] for details). According to the theory, the glassy states for moderately small γ should converge as a power law γ^α to a “threshold” glass that eventually jams at φ_{th} . The dynamical transition density φ_d separates the equilibrium fluid from this glass [25], but at much slower compaction rates $\gamma \lesssim \exp(-d)$ RFOT theory also predicts that activated events allow the system to remain in equilibrium up to higher densities. In this regime we expect a crossover to a logarithmic dependence of the glass EOS on γ (e.g. of the form $1/|\log(\gamma)|$). Eventually, for $\gamma \rightarrow 0$ a true second order phase transition to an “ideal” glass hap-

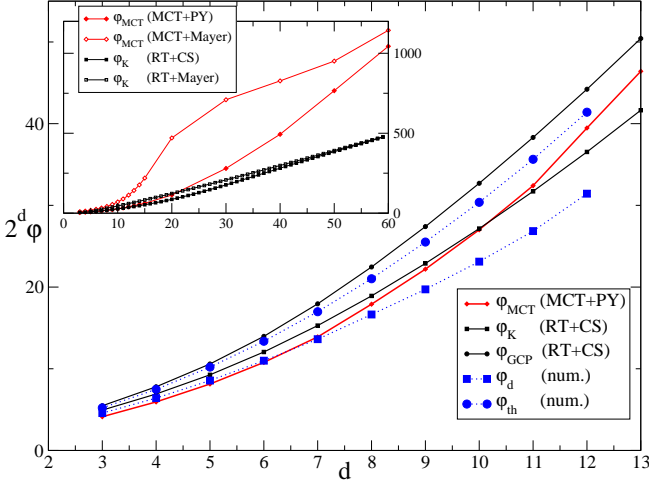


FIG. 2: RFOT critical densities obtained from simulations, RT, and MCT. In the inset, the larger d interval shows the approach to the asymptotic $d \rightarrow \infty$ limit, which happens for $d \approx 60$ in both RT and MCT.

pens at a density φ_K that corresponds to the Kauzmann point. This ideal glass then jams at the glass close-packed density φ_{GCP} . Hence, from this mean-field treatment, stable amorphous packings should exist in the interval $\varphi \in [\varphi_{th}, \varphi_{GCP}]$ [11].

Based on this description, it is clear that the activated regime of RFOT is inaccessible in high dimensions. We therefore focus on the power-law regime and on the threshold glass. In the inset of Fig. 1, the reported $f(\gamma)$ and $\varphi_j(\gamma)$ are both linear as functions of γ^α with $\alpha \approx 0.5$. The exponent is expected to weakly depend on dimensionality, especially at low d , but this value is within the numerically reasonable range for all systems studied. Because the subsequent analysis is rather insensitive to the precise value of α , for simplicity it is kept constant. Extrapolating the results to $\gamma = 0$ gives the parameters φ_{th} and f_{th} for the threshold glass free volume EOS reported in Fig. 1. Its intersection with the fluid EOS then provides a numerical estimate for φ_d . These values are very close to previous numerical estimates in $d = 3$ [26] and $d = 4$ [2], and the results for φ_{th} agree with the results of Refs. [16, 27], which demonstrates the coherence of our analysis in low dimensions. The numerical results reported in Table I and plotted in Fig. 2 further show that the dimensional evolution of φ_{th} and φ_d is smooth. Interestingly, dimensions where the crystal structure is singularly dense, such as $d = 8$ and $d = 12$, do not present any echo of that transition, which illustrates the weak d dependence of the fluid structure.

Theory - The numerical results can also be quantitatively compared with the analytical estimates for the RFOT critical densities. Results for φ_K and φ_{GCP} have been previously obtained by means of RT [11], taking the Carnahan-Starling EOS with parameter A_d^{CS} as input.

d	φ_d	φ_{th}	φ_K (RT+CS)	φ_{GCP} (RT+CS)	φ_{MCT} (MCT+PY)
3	0.571	0.651	0.618	0.684	0.516
4	0.401	0.467	0.432	0.487	0.371
5	0.267	0.319	0.289	0.331	0.254
6	0.172	0.209	0.189	0.219	0.169
7	0.106	0.133	0.120	0.140	0.109
8	0.0650	0.0821	0.0738	0.0875	0.0699
9	0.0385	0.0498	0.0447	0.0535	0.0434
10	0.0226	0.0297	0.0266	0.0319	0.0264
11	0.0131	0.0174	0.0155	0.0187	0.0158
12	0.0077	0.0101	0.00891	0.0108	0.00964
∞			$d \ln d 2^{-d}$	$d \ln d 2^{-d}$	$0.22 d^2 2^{-d}$

TABLE I: Numerical values of the critical densities obtained from the simulations extrapolated at $\gamma = 0$ and the RFOT theories. The uncertainty on the numerical results is on the last reported digit [19].

As we mentioned above, the fitted values A_d^{fit} are slightly different, but that difference only weakly perturbs the results. Because A_d^{fit} is only available for $d \leq 12$, we use instead A_d^{CS} from Ref. [11]. As expected from RFOT theory, $\varphi_K > \varphi_d$ and $\varphi_{GCP} > \varphi_{th}$, and the values follow a similar trend with dimension (Table I).

The MCT analysis follows the approach of Refs. [9, 10] using the Percus-Yevick (PY) structure factor calculated for finite dimension by an iterative method with a numerical Hankel transformation of order $d/2 - 1$. Using instead the hypernetted chain (HNC) input for the structure factor does not strongly affect the results. For the dynamical and static theories to be consistent, the transition density φ_{MCT} predicted by MCT, reported in Table I and plotted in Fig. 2, should coincide with φ_d . It is not the case. The MCT transition at φ_{MCT} increases too fast with dimension and around $d = 13$ will likely cross the numerical estimate of φ_{th} . This situation is paradoxical, because the liquid should fall out of equilibrium well *before* jamming occurs. The usual suggestion that activated events may improve the consistency of the theory by increasing the transition density would here only make things worse.

The inset in Fig. 2 presents φ_{MCT} and φ_K for larger dimensions. Both curves approach the results obtained by neglecting all liquid structure for the liquid [18], which amounts to using the van der Waals' expression $p = 1 + 2^{d-1}\varphi$ for the fluid EOS and the Mayer function $\hat{f}(r) = -\theta(\sigma - r)$ for the direct correlation function [9, 10]. This treatment is exact for $d \rightarrow \infty$, a fact that is also consistent with our simulation results for the fluid EOS. In this asymptotic large d regime, MCT predicts $\varphi_{MCT} \sim 0.22 d^2 2^{-d}$ [9, 10], while RT predicts $\varphi_K \sim d \log(d) 2^{-d}$ [11]. The simulation results at intermediate d thus give convincing evidence that the scaling predicted by MCT is incorrect.

Conclusions - We have presented numerical results that extend previous estimates of the glass transition density [2, 26] and of the amorphous packing density [16] up to $d = 12$. These results are obtained partly thanks to methodological improvements over the approach of Ref. [16]. Reassuringly, our procedure for the data analysis, which is grounded in the RFOT scenario [11], produces results that are consistent with estimates obtained through alternate routes. Two key features arise from the work. First, our numerical estimates of φ_{th} are slightly smaller than the values of φ_{GCP} predicted by RT and follow a similar trend, indicating that RT can provide a reliable prediction for the jamming density of hard spheres in high dimensions. In particular, the random close-packed state of frictionless hard spheres, which is expected to be protocol dependent [11, 28], should fall within the range of densities predicted by the RFOT scenario $\varphi \in [\varphi_{\text{th}}, \varphi_{\text{GCP}}]$. We expect that our numerical results for φ_{th} are thus good estimates of that density, irrespective of the protocol used. Second, our results for the dynamical (glass) transition φ_{d} are slightly smaller than the ideal glass (Kauzmann) transition φ_{K} predicted by RT, as it should be. But at the same time, the MCT prediction φ_{MCT} does not coincide with φ_{d} , unlike what the RFOT scenario suggests. The two quantities additionally show very different trends with dimension and the discrepancy increases at large d . This fact suggests that the standard MCT formulation [6, 9, 10] is not exact at large d , unlike what is expected of a mean field theory. Echoing and amplifying the call of Ref. [9], MCT should therefore be revised.

Mean-field models displaying a RFOT are described by MCT-like equations [4, 7], and MCT itself has been described as a type of Landau theory of the dynamical transition [12, 29]. It is thus probable that a modified MCT with a similar structure might be exact in large d . Steps in this direction have been recently taken [25, 30], although more work is needed. Having a complete RFOT theory that includes both RT and a modified MCT would be an important intellectual advance, as it would be the first complete theory of the glass and jamming transitions for particle-based systems. This advance would open the way towards a more systematic construction of RFOT, through a large d expansion or a renormalization group approach. Some of the uncontrolled physical approximations underlying the construction of MCT might also be more reasonably treated, and lead to a fully predictive glass theory for $d = 3$.

We thank J. Kurchan, R. Mari, K. Miyazaki and R. Schilling for stimulating discussions. PC also acknowledges Duke startup funding.

- [1] P. W. Anderson, *Science* **267**, 1609 (1995).
- [2] P. Charbonneau, A. Ikeda, J. A. van Meel, and K. Miyazaki, *Phys. Rev. E* **81**, 040501(R) (2010).
- [3] J. H. Conway and N. J. A. Sloane, *Sphere Packings, Lattices and Groups* (Springer-Verlag, New York, 1988).
- [4] T. R. Kirkpatrick, D. Thirumalai, and P. G. Wolynes, *Phys. Rev. A* **40**, 1045 (1989).
- [5] M. Mézard and G. Parisi, *Phys. Rev. Lett.* **82**, 747 (1999).
- [6] W. Götze, *Complex Dynamics of Glass-Forming Liquids*, International Series of Monographs on Physics, Vol. 143 (Oxford University Press, Oxford, 2009).
- [7] T. R. Kirkpatrick and P. G. Wolynes, *Phys. Rev. A* **35**, 3072 (1987).
- [8] G. Szamel, *Europhys. Lett.* **91**, 56004 (2010).
- [9] A. Ikeda and K. Miyazaki, *Phys. Rev. Lett.* **104**, 255704 (2010); *Phys. Rev. Lett.* **106**, 049602 (2011).
- [10] B. Schmid and R. Schilling, *Phys. Rev. E* **81**, 041502 (2010); R. Schilling and B. Schmid, *Phys. Rev. Lett.* **106**, 049601 (2011).
- [11] G. Parisi and F. Zamponi, *Rev. Mod. Phys.* **82**, 789 (2010).
- [12] J.-P. Bouchaud, “The mode-coupling theory of supercooled liquids: Does it wear any clothes?” <http://www.condmatjournalclub.org/?p=1022> (2010).
- [13] S. Torquato and F. H. Stillinger, *Exp. Math.* **15**, 308 (2006).
- [14] J. A. van Meel, B. Charbonneau, A. Fortini, and P. Charbonneau, *Phys. Rev. E* **80**, 061110 (2009).
- [15] C. Song, P. Wang, and H. A. Makse, *Nature* **453**, 629 (2008); Y. Jin, P. Charbonneau, S. Meyer, C. Song, and F. Zamponi, *Phys. Rev. E* **82**, 051126 (2010).
- [16] M. Skoge, A. Donev, F. H. Stillinger, and S. Torquato, *Phys. Rev. E* **74**, 041127 (2006).
- [17] In contrast to the original implementation, a canonical definition of temperature is here used, which rescales the time unit ($\beta m \sigma^2$) for particles of unit mass m .
- [18] G. Parisi and F. Slanina, *Phys. Rev. E* **62**, 6554 (2000).
- [19] See Appendix to this paper.
- [20] G. Parisi, *Statistical Field Theory* (Perseus Group, 1998).
- [21] The many virial coefficients known for hard spheres, e.g., Ref. [31], insufficiently capture the equation of state near the onset density of the non-ergodic regime.
- [22] Y. Song, E. A. Mason, and R. M. Stratt, *J. Phys. Chem.* **93**, 6916 (1989).
- [23] A. Donev, S. Torquato, and F. H. Stillinger, *Phys. Rev. E* **71**, 011105 (2005).
- [24] R. D. Kamien and A. J. Liu, *Phys. Rev. Lett.* **99**, 155501 (2007).
- [25] R. Mari and J. Kurchan, [arXiv:1104.3420](https://arxiv.org/abs/1104.3420) (2011).
- [26] G. Brambilla *et al.*, *Phys. Rev. Lett.* **102**, 085703 (2009).
- [27] Within RFOT, the “maximally random jammed” packing discussed in Ref. [16] should be very close to φ_{th} [11].
- [28] F. Krzakala and J. Kurchan, *Phys. Rev. E* **76**, 021122 (2007); S. Torquato and F. H. Stillinger, *Rev. Mod. Phys.* **82**, 2633 (2010).
- [29] A. Andreanov, G. Biroli, and J.-P. Bouchaud, *Europhys. Lett.* **88**, 16001 (2009).
- [30] H. Jacquin and F. van Wijland, *Phys. Rev. Lett.* **106**, 210602 (2011).
- [31] M. Bishop, N. Clisby, and P. A. Whitlock, *J. Chem. Phys.* **128**, 034506 (2008).

* LPTMC, CNRS-UMR 7600, Université Pierre et Marie Curie, boîte 121, 4 Place Jussieu, 75005 Paris, France

Appendix: Details on finite size effects

d	N	A_d^{fit}	A_d^{CS}	$1/p_{\text{min}}$	f_{th}	$2^d \varphi_d$	$2^d \varphi_{\text{th}}$	$2^d \varphi_K$	$2^d \varphi_{\text{GCP}}$	$2^d \varphi_{\text{MCT}}$
			Ref. [22]					(RT+CS)	(RT+CS)	(MCT+PY)
3	8000	0.5	0.5	0.03	0.11(2)	4.57(6)	5.21(1)	4.94	5.47	4.13
4	8000	0.114	-0.051	0.02	0.1175	6.41(6)	7.48(1)	6.91	7.79	5.94
5	8000	-1.086	-1.625	0.02	0.124(5)	8.56(5)	10.20(1)	9.26	10.6	8.13
6	8000	-3.900	-4.910	0.02	0.128(6)	10.98(8)	13.36(2)	12.1	14.0	10.8
7	8000	-9.294	-11.06	0.02	0.130(3)	13.6(1)	16.98(4)	15.3	17.9	13.9
8	1400	-19.38	-22.03	0.02	0.133(6)	16.6(1)	20.98(2)	18.9	22.4	17.9
8	2500	-19.38		0.02	0.135(4)	16.6(1)	21.00(4)			
8	8000	-19.38		0.02	0.136(7)	16.6(2)	21.02(5)			
8	32768	-19.38		0.02	0.14(2)	16.5(3)	20.92(5)			
9	8000	-35.46	-41.10	0.02	0.137(4)	19.7(2)	25.51(7)	22.9	27.4	22.2
10	20000	-62.50	-73.83	0.02	0.139(4)	23.1(2)	30.37(8)	27.2	32.7	27.0
11	50000	-107.0	-129.6	0.015	0.141(2)	26.9(2)	35.64(6)	31.7	38.3	32.4
12	125000	-185.0	-224.3	0.015	0.143(2)	31.4(7)	41.4(4)	36.5	44.2	39.5
∞								$d \ln d$	$d \ln d$	$0.22 d^2$

TABLE II: Numerical values of the RFOT critical densities and of the simulation parameters. The simulation results are extrapolated at $\gamma = 0$ according to the procedure discussed in the text.

Error analysis - From the simulation results, the error on A_d^{fit} is found to be very small and, for all practical purposes, the quantity is here considered exact. While the error on φ_{th} and f_{th} are estimated by taking three times the error on the linear regression coefficients, for φ_d , a standard error propagation is conducted starting from its definition. Indeed φ_d is the intersection of the fluid EOS defined by Eq. (1) and the threshold glass EOS defined by the extrapolation of Eq. (2) to $\gamma = 0$:

$$p_{\text{fluid}}(\varphi) = p_{\text{fv}}(\gamma \rightarrow 0, \varphi) \equiv \frac{d\varphi_{\text{th}}(1 - f_{\text{th}})}{\varphi_{\text{th}} - \varphi}. \quad (3)$$

Defining $q(\varphi) = 1/p_{\text{fluid}}(\varphi)$, we then get that

$$\delta\varphi_d = \left| \frac{1 - d(1 - f_{\text{th}})q(\varphi_d)}{1 + d(1 - f_{\text{th}})\varphi_{\text{th}}q'(\varphi_d)} \right| \delta\varphi_{\text{th}} + \left| \frac{d\varphi_{\text{th}}q(\varphi_d)}{1 + d(1 - f_{\text{th}})\varphi_{\text{th}}q'(\varphi_d)} \right| \delta f_{\text{th}}. \quad (4)$$

Finite-size effects - The finite-size arguments that we presented in the main text are tested by comparing $d = 8$ systems with $N = 1.4\text{K}$, 2.5K , 8K and 32K . Although the number of particles increases by nearly 50% per dimension over this sequence, the compaction curves are almost indistinguishable except for a slight finite size effect for the largest $\gamma = 0.1$. The results of our data analysis coincide within numerical errors, estimated as discussed in the previous paragraph (Table II).